Journal of
Nanomedicine & Nanotechnology

Noori et al., J Nanomed Nanotechnol 2016, 7:4
DOI: 10.4172/2157-7439.1000389

Research Article Open Access

Effect of CO_2 Ion Doping on Characteristics of Nanostructure Hydroxyapatite

Noori A[1], Ziaie F[2]* and Shafaei M[2]

[1]Department of Physics, Taft Branch, Islamic Azad University, Taft, Iran
[2]Radiation Application School, Nuclear Science and Technology Research Institute, Tehran, Iran

Abstract

In this research work, carbonated hydroxyapatite samples with different carbonate contents were prepared using ion implantation method. Pure nano-structure hydroxyapatite samples were implanted by 80 keV CO_2^+ ions during different times of 4, 8, 16, and 24 min using an ion implantation devise. The resulting materials were tested by X-ray diffraction, Fourier transform Infrared spectroscopy, and transmission electron microscopy, electron spin resonance systems before and after the implantation. The results confirmed the doping of carbonate group into the hydroxyapatite structure, and show that the presence of carbonate in the structure of hydroxyapatite decreases the degree of crystallinity. Moreover, it was observed that the increasing of ion implantation time caused to decrease the average grain size of the hydroxyapatite sample.

Keywords: Hydroxyapatite; Ion implantation; Carbonate; FTIR; XRD; TEM; ESR

Introduction

Hydroxyapatite (HAP) is a biocompatible ceramic having the physical and chemical properties similar to the bones and teeth [1,2]. This bio-ceramic have numerous applications including ceramic coating, manufacturing the implants substituted for the bones and teeth, cosmetic foundation [3], radiation dosimetry [4,5] etc. The calcium hydroxyapatite produced by living tissue is called biological HAP. In fact the synthetic type of HAP with the formula of $Ca_{10}(PO_4)_6(OH)_2$ differs slightly from the natural one. Researches show that the biological HAP contains the carbonate groups [6-8] and a small amount of other elements. During the formation of HAP as the hard part of the bones and teeth, some organic groups such as carbonate (CO_3^{2-}) have been replaced over the time in the position of hydroxyl (OH^-) or phosphate (PO_4^{3-}) groups in the HAP crystals. Therefore, they have differences in terms of physical, chemical, mechanical properties as well as their crystallinity, and solubility in comparison to the artificial HAP.

Ion implantation is one of the ways to change the physical structure of thin films. Replacement of ion in the network structure will change the chemical composition of the substrate material, thus other properties of material could be changed subsequently. In this method, high-energy ions produced by an ion implantation device with perfect vacuum penetrate into the substrate material. Planted ions may lead to three processes within the material that are: scission of primary bond and replacement of network atoms, entering the channel (space between the structure), and locating the position of network defects [9,10].

In the present work the CO_2^+ ions entered into the HAP crystal structure in different implantation times and the changes in structure were studied and compared.

Materials and Methods

Sample preparation

Polyvinyl alcohol (PVA) powder (2 w%) was dissolved in water at room temperature, to prepare an adhesive solution. The resulted glue was mixed with HAP powder prepared from Merck Company. The produced paste was kept for two days in air evacuated nylon to agglomerate and become suitable to use. The obtained substance was milled for half an hour to obtain a smooth and homogeneous powder. Then the pill shape samples with 13 mm in diameter were prepared using a hydraulic press, punch and matrix made of non-corrosive alloy under 700 MPa.

Ion implantation procedure

The prepared pills without any hand contact and using the cleaned tools were transferred to the special sample place in the ion implantation system. Before each implanting operation, the chamber was scoured out with alcohol and acetone. When the vacuum pressure reached to 2×10^{-5} Torr, the valve connected to the CO_2 gas capsule was opened till the vacuum reached the desired values (Table 1). Then the appropriate voltage and current were applied to produce an 80 keV CO_2^+ ion beam. The samples were exposed to the ion beam in different time periods of 4, 8, 16 and 24 min. All the system parameters during the ion implantation are depicted in Table 1. An ion implantation system model MBM100, made in China was used in this research work.

Characterization

Fourier transmission infrared spectroscopy (FTIR) was carried out in the wave number range of 400-4000 cm^{-1} using a Perkin Elmer, series 100 spectrometer.

System parameters	Sample 1	Sample 2	Sample 3	Sample 4
implantation time (s)	240	480	960	1440
Ion beam current (mA)	16	18	18	20.5
Beam voltage (kV)	80	80	78	83
Vacuum Pressure (2×10^{-5} Pa)	3.7	3.2	3.2	3.7
Beam current on sample (μA)	0.5	0.5	0.5	0.5

Table 1: Ion implantation system parameters.

***Corresponding author:** Farhood Ziaie, Nuclear Science and Technology Research Institute, Tehran, Iran, Tel: 202-223-8299; E-mail: fziaie@aeoi.org.ir

Received June 07, 2016; **Accepted** July 11, 2016; **Published** July 18, 2016

Citation: Noori A, Ziaie F, Shafaei M (2016) Effect of CO_2 Ion Doping on Characteristics of Nanostructure Hydroxyapatite. J Nanomed Nanotechnol 7: 389. doi:10.4172/2157-7439.1000389

X-ray diffraction (XRD) analysis was performed by a Philips Analytical X-Ray B.V., using the Cu-K_α radiation (1.5456 Å wavelength), in 2θ range of 20°-60°. The grain size of the prepared products was calculated using the Scherer's equation indicated as below:

$$t(nm) = (0.89 \times \lambda(nm)) / (B(rad) \times cos\theta)$$

where t is sample grain size, λ is the X-ray wavelength, B is full width at half maximum of a peak in the X-ray pattern, and θ is the Bragg's angle.

Transmission electron microscopy (TEM) studies were also carried out using a Zeiss EM10C microscope at 80 kV.

ESR measurement

Electron spin resonance (ESR) spectroscopy is an extremely sensitive method for studying materials containing unpaired electrons. The samples were put into the quartz thin-wall ESR tubes (4 mm diameter) and measured with a Bruker EMS-104 spectrometer operating in x-band. The ESR signal intensities were measured as peak to peak height for the most intense ESR lines (first derivative of the absorption spectra) per sample mass. The used ESR spectrometer parameters for this study were 0.285 mT modulation amplitude, 100 kHz modulation frequency, 3.0 mT scan width, 1024 point field resolution, 164 msec time constant, 21 sec sweep time, and 50 dB receiver gains.

Result and Discussions

Figure 1 shows the XRD patterns of the samples were implanted at different times in comparison to the non-implanted one. Evaluation and comparison of the diffraction patterns before and after the implanting indicate the existence of the peaks in all samples which are fully in accordance with the standard cards of hydroxyapatite (card no. 00-0350-0180). Among these peaks, the Miller indices of the most intense 9 peaks are indicated in the figure. The XRD patterns show that the peak positions before and after implantation have not changed and no new peak appeared afterward. Considering the intensity of the peak in position of 25.9° with Miller indices of (002), it is obvious that an increase in implantation time (carbon increase), decreases the peak height and increases the peak width as shown in Figure 2. This result is in agreement with those reported in some references [11-15].

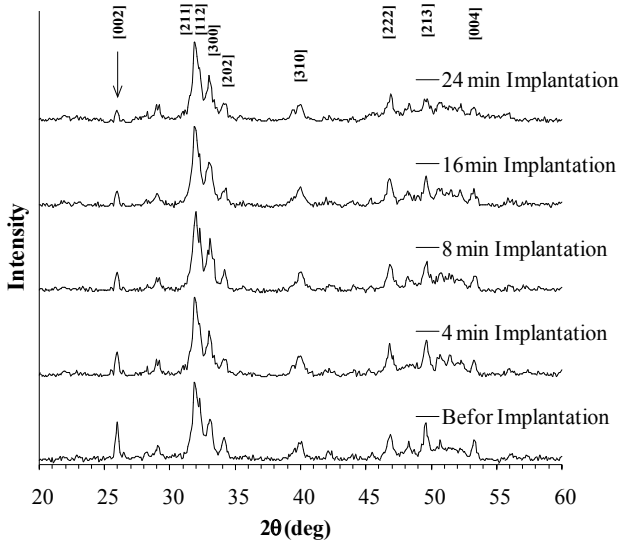

Figure 1: XRD patterns of the HAP samples implanted with CO_2^+ ions at different times in comparison to the non-implanted one (Miller indices are shown for the main peaks).

Therefore, it can be concluded that shortening the peak height and increasing the peak due to intensification of the implantation time, will be followed by crystallinity reduction. This variation was calculated and given in Table 2 and shown in Figure 3.

Figure 4 shows the FTIR analysis results for the samples before and after the implantation. All of the observed bands are related to the carbon apatite which can be arranged in three types of phosphate, carbonate and hydroxyl groups. A broad band in position of 1043 cm^{-1} and two narrow bands in positions of 567 cm^{-1} and 603 cm^{-1}, and another one in position 962 cm^{-1} are related to the phosphate compounds. Two bands in positions 603 cm^{-1} and 1051 cm^{-1} are also reported for phosphate compounds. The bands were observed in positions of 883 cm^{-1} and 1417 cm^{-1} till 1576 cm^{-1} were associated with carbon compounds that

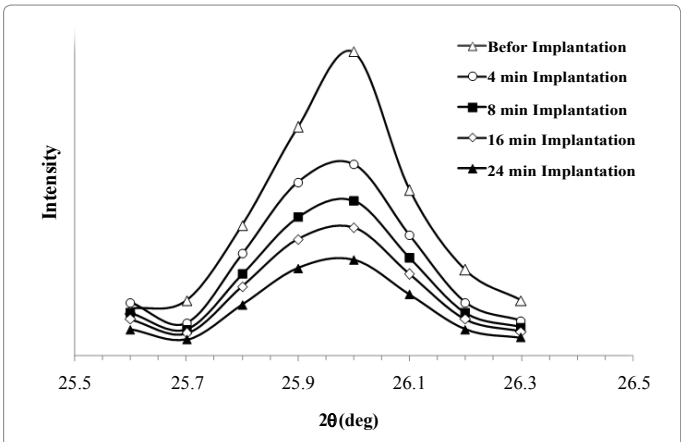

Figure 2: XRD patterns of the HAP samples implanted with CO_2^+ ions in different scales (for peak of [002]).

Implantaion time	Peak position	Peak width	Peak height
0 min	25.981°	0.19 6°	149
4 min	26.022°	0.198°	94
8 min	25.985°	0.275°	76
16 min	25.947°	0.305°	63
24 min	25.952°	0.332°	47

Table 2: Data related to (002) peak.

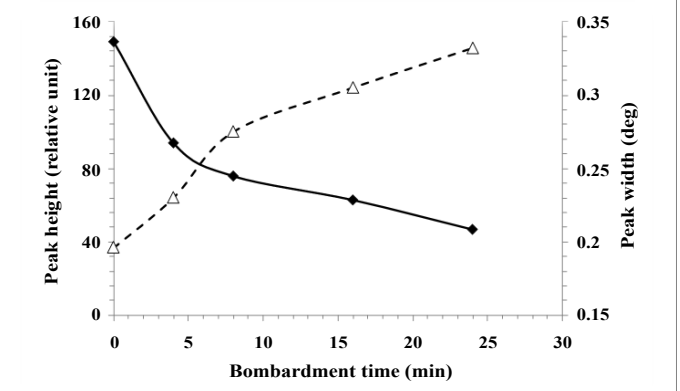

Figure 3: Variation of 002 associated peak heights and widths as a function of implantation time.

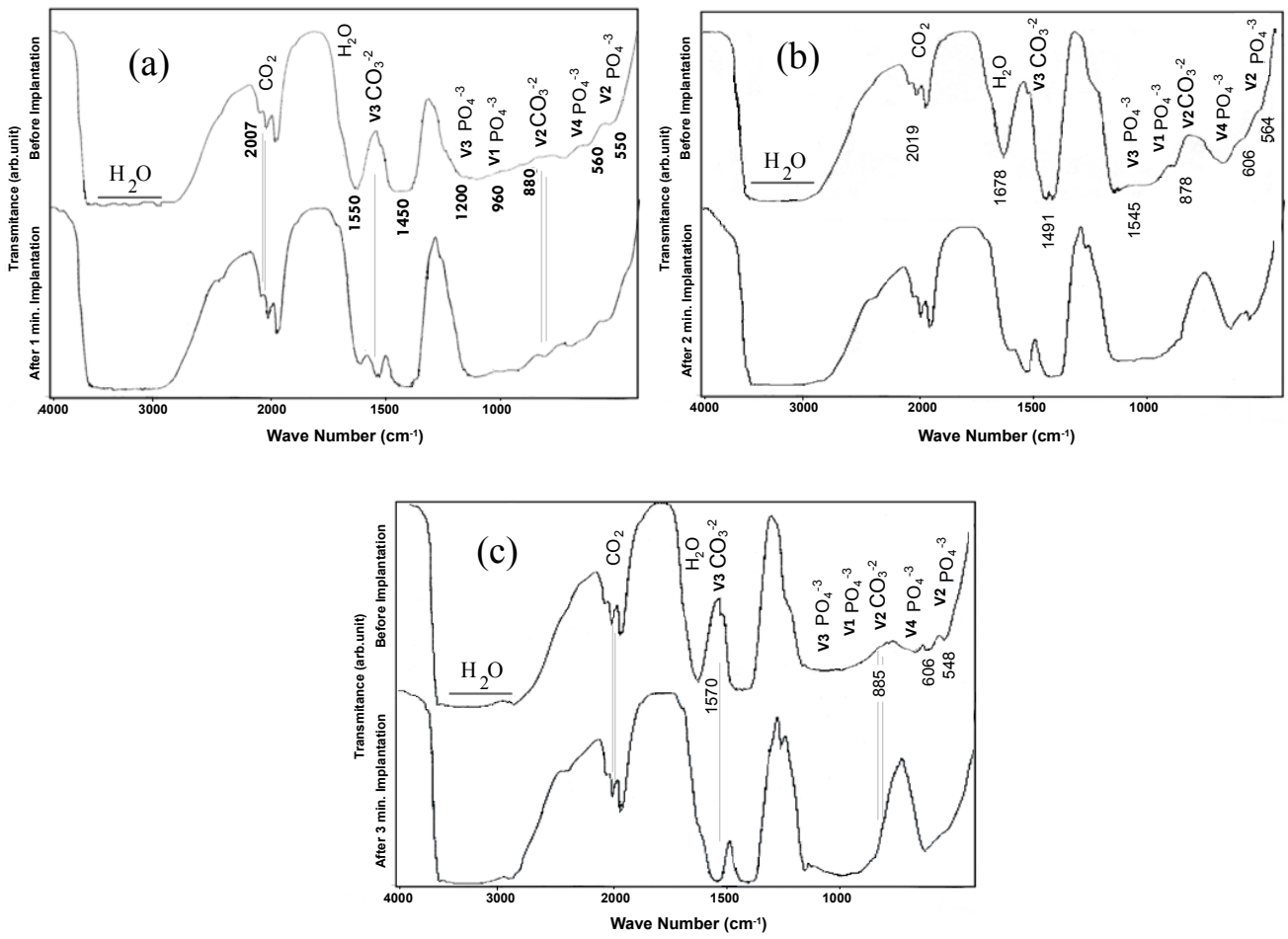

Figure 4: FTIR spectrum of CO_2 ions implanted samples in different time periods of, a) 4 min, b) 8 min, c) 16 min, in comparison to the non-implanted one.

became more intense by increasing the implantation time. This means that the carbon entered in to the structure of hydroxyapatite samples via this method. Another broad band around the position of 3436 cm^{-1} was related to the hydroxyl ions (water) which means that the samples containing little water were probably related to the production stage of the pills [15].

Chemical structure of the hydroxyapatite and CO_2^+ ion is shown in Figure 5 [13]. According to this figure, the CO_2^+ ions can enter into the channels or bonds with the oxygen in one of the two indicated positions, and eventually form carbon apatite.

Therefore, it can be concluded that the ion implantation technique is a physical method to insert the carbonate group into the structure of hydroxyapatite, which it leads to the production of carbon apatite. Also, in this method the implantation time, sample moisture content, and the ion energy can be considered as the process variables to improve the result.

The grain sizes of the HAP samples were calculated via equation 1 using the data extracted from the XRD patterns for the main XRD peaks. The averages over the same implantation time are reported in Table 3.

These calculations were done via fitting the Gaussian function to each single peak and calculating their overlap, with respect to the position and peak widths. The indicated standard deviation means that there is a distribution over the particle sizes in each set of the HAP

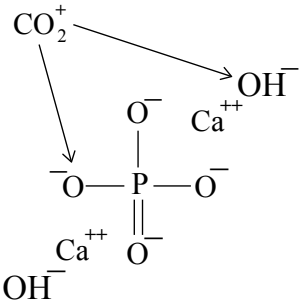

Figure 5: Expanded schema of the hydroxyapatite and the manner of bonding with CO_2^+.

Implantation time	Average particle size
0 min	22.24 ± 3.17 nm
4 min	21.19 ± 3.51 nm
8 min	19.22 ± 2.61 nm
16 min	18.66 ± 2.51 nm
24 min	17.98 ± 2.82 nm

Table 3: Average grain sizes of the HAP samples implanted in different times.

samples. These results demonstrate that the average grain size decreases while the ion implantation time increases. In the author's view the decreasing of sample grain sizes is associated with the sputtering of grains due to the hitting of accelerated carbon ions. In fact, an increase in implantation time causes more spattering and a smaller particle size. TEM micrographs of the HAP samples are demonstrated in Figure 6. The particle sizes in the samples are obvious in TEM-associated image which confirms the obtained results indicated in Table 3.

Figure 7 shows the ESR responses of the samples after different ion implantation times. According to this figure, the ESR signal increases strongly after 4 min ion implantation as a result of carbon ion incorporation into HAP crystal, and remained approximately constant at the higher implantation time.

In fact the carbonated impurities are incorporated into, or attached to the surface of HAP crystal during formation, and are converted to radicals through absorption of ionizing radiation. Thus, the non-implanted sample, do not show an intensive ESR response where this response value could be due to the native or mechanical induced signals. At the higher implantation time the amount of induced radicals remains constant due to the fact that the carbonate ions mostly contribute in sputtering of the particles and loss their energy afterwards. It means that the saturation occurs after a few minutes of implantation.

Conclusions

The FTIR analysis indicates that as carbon entered into the structure of HAP the carbon apatite was formed. Increasing the implantation time decreases the (002) peak height and increases the peak width in the XRD patterns of the HAP samples which means crystallinity reduction.

The obtained results from the XRD and TEM analyses demonstrate that the average grain size decreases while the ion implantation time increases. Therefore, the ion implantation technique is a physical method to insert the carbonate group into the structure of HAP and it leads to the production of carbon apatite.

The EPR response of the HAP samples implanted by carbonate ions show the higher intensities in comparison to non-implanted sample. But the saturation occurs after a few minutes of implantation.

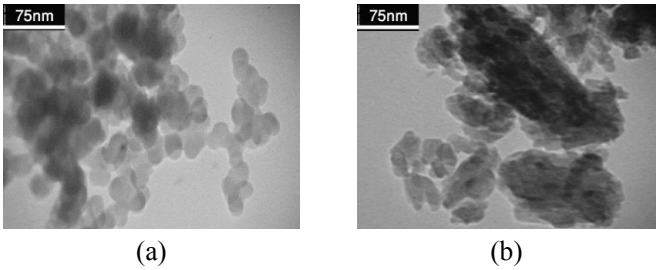

Figure 6: Magazine logo TEM provided microstructure of HAP samples a) before implantation and b) implanted with CO_2^+ ions in 24 min.

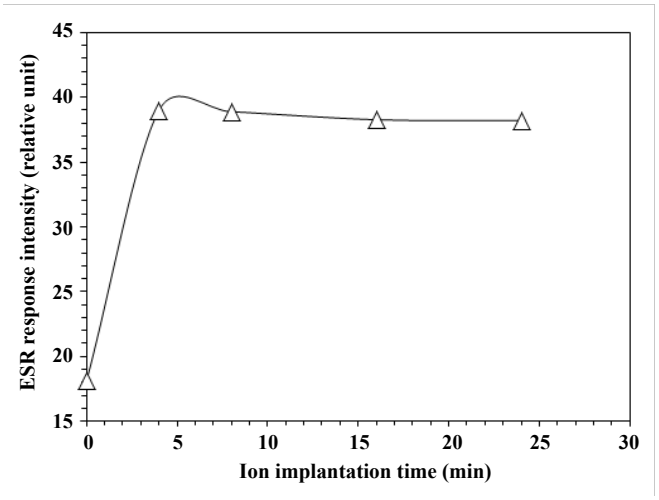

Figure 7: ESR responses of ion implanted samples after different implantation time.

References

1. Lakes RS, Joon P (2007) Biomaterials: an introduction. Springer.
2. Baghalzadeh B, Ziaie F, Dowlatshah F, Larijani M (2013) Gamma irradiated EPR response of carbonate ion implanted hydroxyapatite. Nuclear Technology and Radiation Protection 28: 260-264.
3. Iwasaki T, Nakatsuka R, Murase K, Takata H, Nakamura H, et al. (2013) Simple and rapid synthesis of magnetite/hydroxyapatite composites for hyperthermia treatments via a mechanochemical route. International journal of molecular sciences 14: 9365-9378.
4. Ziaie F (2014) CO_2 doped γ-irradiated hydroxyapatite for EPR dosimetry. Kerntechnik 79: 446-450.
5. Shafaei M, Ziaie F, Sardari D, Larijani M (2015) Study on carbonated hydroxyapatite as a thermoluminescence dosimeter. Kerntechnik 80: 66-69.
6. Aoki H (1994) Medical applications of hydroxyapatite. Ishiyaku EuroAmerica Incorporated.
7. Ratner BD, Hoffman AS, Schoen FJ, Lemons JE (2004) Biomaterials science: an introduction to materials in medicine. Academic press, Elsevier Store.
8. Epple M, Bäuerlein E (2008) Medical and clinical aspects Weinheim: Wiley-VCH.
9. Driessens F (1980) The mineral in bone, dentin and tooth enamel. Bulletin des sociétés chimiques belges 89: 663-689.
10. Callens F, Vanhaelewyn G, Matthys P, Boesman E (1998) EPR of carbonate derived radicals: Applications in dosimetry, dating and detection of irradiated food. Applied magnetic resonance 14: 235-254.
11. Schramm DU, Rossi AM (2000) Electron spin resonance (ESR) studies of CO2-radicals in irradiated A and B-type carbonate-containing apatites Appl Radiat Isot 52: 1085-1091.
12. De Oliveira L, Rossi A, Lopes R (2001) Dose response of A-type carbonated apatites prepared under different conditions. Radiation Physics and Chemistry 61: 485-487.
13. Suchanek WL, Shuk P, Byrappa K, Riman RE, TenHuisen KS et al. (2002) Mechanochemical–hydrothermal synthesis of carbonated apatite powders at room temperature. Biomaterials 23: 699-710.
14. Liao S, Watari F, Xu G, Ngiam M, Ramakrishna S, et al. (2007) Morphological effects of variant carbonates in biomimetic hydroxyapatite. Materials Letters 61: 3624-3628.
15. Pieters IY, Van den Vreken NM, Declercq HA, Cornelissen MJ, Verbeeck RM (2010) Carbonated apatites obtained by the hydrolysis of monetite: influence of carbonate content on adhesion and proliferation of MC3T3-E1 osteoblastic cells. Acta Biomater 6: 1561-1568.